JOURNAL OF AIRCRAFT
Vol. 29, No. 3, May–June 1992

Design Optimization of Natural Laminar Flow Bodies in Compressible Flow

Simha S. Dodbele*
ViGYAN, Inc., Hampton, Virginia 23666

An optimization method has been developed to design axisymmetric body shapes such as fuselages, nacelles, and external fuel tanks with increased transition Reynolds numbers in subsonic compressible flow. The new design method involves a constraint minimization procedure coupled with analysis of the inviscid and viscous flow regions, and linear stability analysis of the compressible boundary layer. In order to reduce the computer time, boundary-layer transition is predicted by Granville's transition criterion to calculate the gradients of the objective function and linear stability theory coupled with the e^n method are used to calculate the functional value at the end of each design iteration. A tip-tank of a business jet is used to illustrate that the method can be utilized to design an axisymmetric body shape with extensive natural laminar flow. Boundary-layer transition is predicted to occur at a transition Reynolds number of 6.04×10^6 on the original tip-tank. On the designed body shape, a transition Reynolds number of 7.22×10^6 is predicted using compressible linear stability theory coupled with e^n method.

Nomenclature

A/A_0 = ratio of local disturbance amplitude to amplitude at the point of neutral stability for a fixed disturbance frequency
C_D = body drag coefficient (based on frontal area)
C_p = pressure coefficient
f_{obj} = objective function
f_r = fineness ratio (body length/maximum body diameter)
L = body length, ft
M = freestream Mach number
NLF = natural laminar flow
n = logarithmic exponent of amplitude-growth ratio of unstable Tollmien-Schlichting wave, $n = \ell n(A/A_0)$
R_L = Reynolds number based on freestream conditions and body length
R_{tr} = Reynolds number based on freestream conditions and transition length
R' = unit Reynolds number based on freestream conditions
$T\text{-}S$ = Tollmien-Schlichting
$T(y)$ = boundary-layer temperature profile
$U(y)$ = boundary-layer velocity profile
V = volume of the body, ft^3
X = axial coordinate starting at nose, ft
X_{tr} = axial coordinate of transition starting at nose, ft
x = nondimensional axial coordinate, X/L
x_{tr} = nondimensional axial coordinate of transition, X_{tr}/L
$x_{tr}(g)$ = nondimensional transition location by Granville's criterion
$x_{tr}(e^n)$ = nondimensional transition location by e^n method
ψ = obliqueness of $T\text{-}S$ disturbances with respect to streamlines, deg

Introduction

RECENT advances in airplane construction techniques and materials employing bonded and milled aluminum skins and composite materials allow for the construction of aerodynamic surfaces without significant waviness and roughness, permitting long runs of natural laminar flow (NLF) over wings in subsonic flow. These advances lead to excellent opportunities for airplane drag reduction by increasing the extent of NLF over wings.[1] As compared to lifting surfaces, laminar flow research on nonlifting air-frame surfaces, such as fuselages, nacelles, and external fuel tanks has received limited attention.[2,3] Substantial drag reduction can be obtained by increasing the extent of laminar flow on the nonlifting surfaces.

Reference 3 presents a recent overview of incompressible transition experiments on axisymmetric body shapes. References 4–6 present results of incompressible, underwater transition experiments over bodies of revolution with varying fineness ratios indicating maximum transition Reynolds numbers of about 20 million. A recent study[7] of bodies of revolution in high subsonic speeds without supersonic regions (subcritical flow) demonstrated the potential for tripling the length of sufficiently stable laminar flow at Mach number (M) = 0.8 and length Reynolds number (R_L) = 40×10^6, in comparison with incompressible speed at the same length Reynolds number. A transition experiment was conducted in the NASA Ames 12-ft pressure tunnel by Boltz et al.[8,9] at high subsonic freestream Mach numbers, measuring the transition locations in two ellipsoids of fineness ratios (f_r) of 7.5 and 9.14. Transition occurred around the location 80–88% of the length of the body at M = 0.90–0.96. Reference 10 presents correlation of compressible boundary-layer-stability results for several of the experimental results reported in Ref. 8 and indicates that integrated $T\text{-}S$ linear logarithmic amplification factors (n factors) of 8–11 are correlated at the point of measured transition onset.

The transition process over an axisymmetric body shape is caused by large amplitude growth of Tollmien-Schlichting ($T\text{-}S$) disturbance waves in the laminar boundary-layer flow. In compressible flow, the presence of density gradient in the boundary layer in the direction normal to the wall in addition to the velocity gradients can result in a large reduction in the spatial growth of $T\text{-}S$ disturbances in the laminar boundary layer. The favorable damping effect of the $T\text{-}S$ waves in compressible flow contribute to the achievement of increased transition-Reynolds numbers on lifting as well as nonlifting aircraft surfaces in the absence of crossflows.[7] This favorable effect of compressibility should be exploited in the design of advanced NLF bodies for application to general aviation, commuter, transport aircraft, and business jets.

Presented as Paper 90-0303 at the AIAA 28th Aerospace Sciences Meeting, Reno, NV, Jan. 8–11, 1990; received April 2, 1990; revision received April 4, 1991; accepted for publication April 27, 1991.

*Research Scientist. Senior Member AIAA.

This paper presents a design method to generate body shapes with increased transition Reynolds numbers at subsonic compressible speeds. In Refs. 2 and 3, it was indicated that a transition-prediction criterion based on linear boundary-layer stability theory coupled with the e^n method (originally introduced by Smith[11] and Van Ingen[12] seems to be a more reliable approach to predict onset of transition in the design of *NLF* fuselages.[13-16] However, the prediction of onset of transition using linear stability analysis coupled with the e^n method alone (hereafter referred to as the e^n method) in the design method will be very expensive and time consuming. A new approach was formulated in the design method in which Granville's transition[17] criterion was used for predicting the gradients of the objective function in the design calculations and the e^n method was used only while predicting the objective function at the end of each iteration. This new approach, based on Granville's transition criterion, and a transition criterion based on the e^n method could be more practical in the design calculations. Design calculations performed for a tip-tank in compressible subsonic flow are presented as a case example.

Optimization Procedure for *NLF* Body Design

The design method developed to obtain body shapes with extensive runs of laminar flow is illustrated in the flowchart (Fig. 1). Initial values of the design variables describing the body shape are input along with the length Reynolds number, Mach number of the freestream, and the fineness ratio of the desired body shape. The axisymmetric body is described by design variables representing the body ordinates in the forebody section and in the aftbody section. By having a large number of design variables in the forebody region, the forebody can be represented in great detail especially near the nose region[18] and small body perturbations dictated by the design cycles can be incorporated.

Several methods are available for optimization in engineering applications, e.g., the constrained-minimization method,[19] the quasi-Newton's method,[20] and the evolution method.[21] The constrained-minimization method developed by Vanderplaats (CONMIN)[19] has been used in the present investigation because of its easy accessibility. The constrained-minimization method is coupled with analysis of the inviscid and viscous flow regions, linear stability analysis of the compressible boundary layer and a transition prediction method.

The aerodynamic analysis program used in the present optimization procedure is based on a low-order surface-singularity method (VSAERO).[22] Pressure distributions and velocity distributions are computed by this aerodynamics program, which uses surface singularity panels to represent the body shape. The boundary-layer profiles along the surface of the body, required for the e^n method, are generated by a modified axisymmetric boundary layer code (VGBLP).[23] The finite-difference program calculates detailed boundary-layer velocity and temperature profiles along with their first and second derivatives normal to the surface, including the effects of transverse curvature. Analysis of the laminar boundary-layer stability along the body is done using a compressible linear stability method. The COSAL program[24] solves the finite difference boundary-layer stability equations by using matrix methods. The compressible *T-S* eigenvalue problem is solved for each boundary-layer station along the body surface giving temporal growth rates of the instability waves propagating at specific wavelengths and wave angles. The temporal growth rates are transformed to the spatial growth rates using Gaster's phase-velocity relationship.[25] Boundary-layer transition is predicted by the e^n method in which n, usually referred to as n factor, is obtained by integrating the linear growth rate of the *T-S* waves from the neutral stability point to a location downstream of the body.

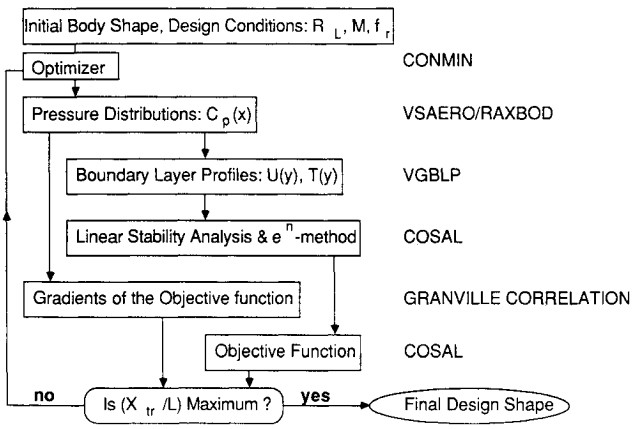

Fig. 1 Flowchart of design procedure for *NLF* fuselage.

The correlation of a large number of wind-tunnel data and flight transition experiments with linear boundary-layer stability calculations has made the e^n method a consistent transition-prediction method (see Ref. 15). For experiments in wind tunnels with low turbulence and low acoustic levels, the onset of transition can be correlated with a n factor of 9–11 in subsonic, transonic, and supersonic flows. In the case of flight tests, higher n factors of the order of 12–15 have been correlated with transition onset.

A number of geometric and aerodynamic constraints are imposed on the design parameters to generate practical and realistic body shapes for given design conditions. Judicious choice of the upper and the lower bounds for the design variables will accelerate convergence of the solutions. The level and the location of the minimum surface pressure along the body surface are aerodynamically constrained by the requirement that the turbulent boundary layer over the aft portion of the body should not separate until $x = 0.95$ for the design conditions.

The objective function is taken to be a function of the location of transition as follows:

$$f_{\text{obj}} = 1 - x_{\text{tr}}(g)$$

for calculating gradients of the objective function

$$f_{\text{obj}} = 1 - x_{\text{tr}}(e^n) \tag{1}$$

for calculating the objective function from a proposed set of design variables at the end of each iteration, where

$$x_{\text{tr}}(g)$$

is the transition location predicted by using Granville's transition criterion and

$$x_{\text{tr}}(e^n)$$

is the transition location predicted by using e^n method with a n factor of 9.

In the optimization calculations described in Ref. 2, the drag coefficient was chosen as the objective function. Because, in the present design method, the location of transition appears explicitly in the objective function, it is possible to derive a body optimized for *NLF* directly. The objective function given by Eq. (1) is to be minimized subject to the constraints on the design variables. The optimizer computes gradients of the objective function using Granville's transition criterion and then, using either a conjugate-direction method or a method of feasible direction, determines a linear search direction, along which a new constrained variable is constructed.

An improved or minimum feasible objective functional value is calculated by using e^n method transition criterion given by Eq. (1) and a series of proposed updated design variables are calculated. The objective function and the constrained func-

tion are evaluated using the updated design variables, interpolating over the range of feasible proposed design variables resulting in a minimum value of the objective function. The results are tested for a convergence criteria. The procedure will stop if the convergence criterion is satisfied, giving a body shape with maximum transition length satisfying the separation constraint. If the convergence criterion is not satisfied, the design parameters go through the analyzer again resulting in a new set of design variables and the procedure is repeated until a final body shape is obtained.

Computational Results and Discussions

Results obtained by the optimization procedure are discussed through an example. All the computations were done on a CRAY-2 computer. A body of revolution whose maximum diameter and length corresponds to those of a tip-tank of a representative business aircraft is considered. The tip-tank has a fineness ratio of 8 and the design flight conditions considered for the present calculations are given by $M = 0.7$, zero incidence and $R' = 1.28 \times 10^6$/ft. In the present example, a n factor of 9 is assumed for prediction of the onset of transition.

At zero incidence, the growth of the two-dimensional T-S disturbances is the most dominant instability mechanism on an axisymmetric body leading to transition in the boundary layer if laminar separation does not happen earlier than natural transition. Crossflow instability can develop on the body at nonzero angles of attack. These crossflow vortices can interact with T-S waves and may lead to premature transition. Such complex three-dimensional boundary-layer flows are the subject of current boundary-layer transition investigations and are not considered here.

The axisymmetric body is modeled by a set of 27 body coordinates with 12 points defining the forebody section and 15 points defining the aftbody section. For the aerodynamic analysis, the body is modeled by 32 panels in the axial direction and 8 panels in the circumferential direction representing the axisymmetric body by a total of 256 panels. It was found that the present choice of the number of panels produces reasonably accurate inviscid pressure distribution by the VSAERO method. The boundary-layer velocity and temperature profiles are obtained at 101 points in the direction normal to the surface and at 90 stations in the streamwise direction. Presently, in the design method the boundary-layer calculations are carried out for adiabatic wall conditions and zero suction through the wall.

The boundary-layer stability equations for the example considered are solved at every fifth streamwise boundary-layer station starting from the first station, although it is possible to perform the boundary-layer stability calculations at every axial boundary-layer station. The boundary-layer stations are skipped from the point of view of reducing the computational time and it has been observed that this reduction in the number of boundary-layer stations for stability calculations does not change the overall results and the conclusions drawn in this investigation. In the global search for eigenvalues, the sixth-order stability equation obtained by neglecting dissipation terms in the boundary-layer stability equations is solved at each chordwise station and in the local search for the eigenvalues the full eighth order stability equation is solved.

Figure 2 presents the pressure distribution on the baseline tip-tank and the results of the compressible linear stability analysis for several T-S disturbance frequencies. The pressure coefficients remain subcritical on the entire body. The figure shows that the most critical disturbance reaching a n factor of 9 has a frequency in the neighborhood of 3500 Hz. Transition onset is predicted to occur for this tip-tank shape at $x_{tr}(e^n) = 0.33$ ($R_{tr}(e^n) = 6.04 \times 10^6$).

Twelve design variables representing the ordinates in the forebody region are allowed to vary within the set of specified upper and lower bounds while simultaneously holding the tail section aft of the maximum thickness point unchanged during

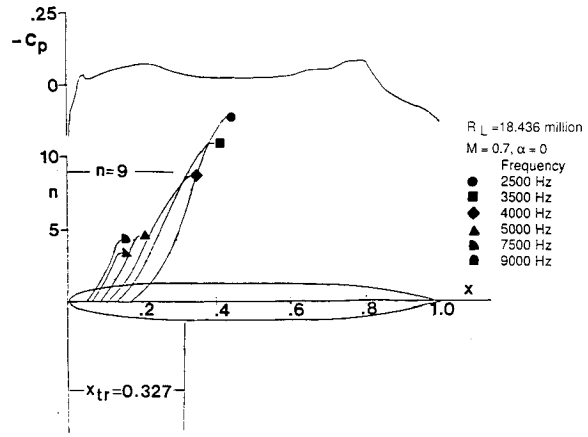

Fig. 2 Pressure distribution and predicted compressible T-S disturbance growth curves and transition on the original tip-tank.

the design iterations. The obliqueness of the T-S waves with respect to the streamlines (ψ) in pure axisymmetric flow does not occur until the local flow speed exceeds the local sonic speed. In the present example, because the axisymmetric flow is subcritical $\psi = 0$ deg is assumed in the design calculations. Prior knowledge of the critical boundary-layer disturbance frequencies, which are functions of the Mach number, helps to identify the critical frequency spectrum during the course of the design optimization. In general, the spectrum of T-S disturbance frequencies should be chosen such that it does not exclude any disturbance frequencies that may grow substantially on a new body shape generated during the design iterations. In the present example, the body shapes do not go through sufficiently large perturbations as the number of iterations increase and, hence, the initially chosen set of T-S frequencies contains all the growing disturbances throughout the design calculations. The same set of T-S disturbance frequencies that are used in the linear stability analysis for the original tip-tank is used in the design optimization.

The present formulation of the stability Eq. (24) does not include transverse-curvature effects and the effect of streamline divergence (i.e., T-S wave stretching in the nose region, generally termed *vortex stretching*).[26] In general, transverse surface curvature has a slightly stabilizing influence on T-S disturbance growth if the curvature is large in relation to the thickness of the boundary layer.[27] During the course of the design calculations, concave curvature may develop on the axisymmetric body. It is known that centrifugal instabilities in the form of Görtler vortices occur in the shear flow over concave surfaces.[28,29] In the present boundary-layer stability calculations, the effect of the centrifugal instabilities are not considered. The design program took 2785 s to predict the final design shape.

The original tip-tank and the final body shape obtained using the design method along with the results of stability analyses are shown in Fig. 3 for comparison. The envelope for the new body shape has a smaller gradient than that on the original tip-tank shape. On the original tip-tank, high-frequency disturbances (5000, 6000, and 7500 Hz) grow up to about 20% of the axial body length from the nose and then become stable. These high-frequency disturbances do not grow beyond a n factor of 5. The critical disturbance characterized by a frequency of 3500 Hz starts growing after 13% of the body length from the nose and reaches a n factor of 9 at $x_{tr}(e^n) = 0.33$ ($R_{tr}(e^n) = 6.04 \times 10^6$).

On the modified body the disturbances with frequencies of 3500 Hz and 4000 Hz do not grow as much as they grow on the original tip-tank. The disturbance frequency of 9000 Hz, which does not grow at all on the original tip-tank, grows on the new body until a n factor of about 6 is reached. The disturbance with a frequency of 2500 Hz does not grow at all on the designed body shape and the disturbance with the same

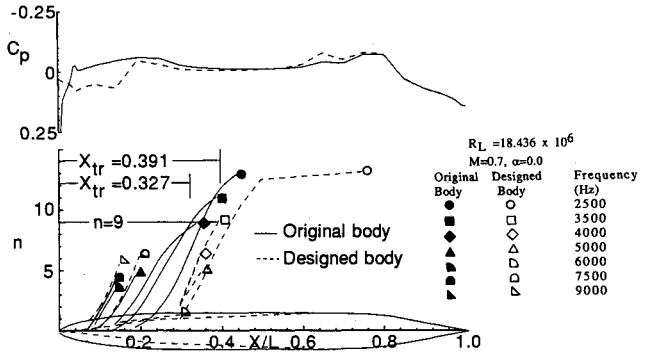

Fig. 3 Pressure distributions, predicted compressible *T-S* disturbance growth curves and transition locations on the original tip-tank and the final design shape.

frequency grows to a n factor of about 13 in the case of the original tip-tank. The transition location corresponding to n factor of 9 occurs at $x_{tr}(e^n) = 0.39$ ($R_{tr} = 7.22 \times 10^6$) on the designed body. Although the critical frequency leading to transition remains at 3500 Hz on the original tip tank and the designed body, boundary-layer transition corresponding to a n factor of 9 as predicted by the e^n method occurs much further downstream on the designed body.

To assess the effect of extending the length of laminar boundary-layer flow over the geometries analyzed, calculation of the viscous drag is made using a modified integral boundary layer approach.[3] An improved turbulent boundary-layer calculation method is incorporated in the panel method to give more realistic drag calculations with available experimental data. The turbulent boundary-layer calculations are based on Head's entrainment method as modified by Shanebrook and Sumner.[30] Validation of this improved method with experimental drag measurements by Gërtler[31] on axisymmetric turbulent body shapes at R_L of 10.0×10^6 and 26.0×10^6 shows that the drag coefficient can be calculated accurately for these predominantly turbulent flow geometries.[3] A drag coefficient (C_D) of 0.0491 is predicted on the original tip-tank with boundary-layer transition at $x_{tr} = 0.33$ and a drag coefficient (C_D) of 0.0415 is predicted on the designed body shape with transition at $x_{tr} = 0.39$.

The designed body shape has a very small nose radius. Nose shapes with extremely small nose radii will produce large pressure peaks at nonzero angles of attack. A constraint on the nose radius will help alleviate the off-design aerodynamic characteristics.

Concluding Remarks

An optimization procedure was developed to design axisymmetric body shapes with increased transition Reynolds number. The design method involved a constraint-minimization procedure coupled with analysis of the inviscid and viscous flow regions, and linear stability analysis of the compressible boundary layer. Granville's criterion was used to compute all the gradients required by the constrained-minimization method. At the end of each iteration, an objective function was predicted by transition criterion based on e^n method. This new approach of evaluation of the objective function would be more practical and would save more computer time than would the approach in which e^n method is used for all the transition predictions in the design method.

A tip-tank of a business jet was chosen as an example to demonstrate that the method could be used to design an axisymmetric body shape with increased transition Reynolds number. Boundary-layer transition was predicted to occur at a transition Reynolds number of 6.04×10^6 on the original tip-tank. On the designed body shape, a transition Reynolds number of 7.22×10^6 was predicted using the e^n method, an increase of 20% in transition Reynolds number.

Acknowledgment

The research was supported by NASA Langley through Grant NAS1-18585.

References

[1]Holmes, B. J., Obara, C. J., and Yip, L., "Natural Laminar Flow Experiments on Modern Airplane Surfaces," NASA TP-2256, June 1984.

[2]Dodbele, S. S., Van Dam, C. P., and Vijgen, P. M. H. W., "Design of Fuselage Shapes for Natural Laminar Flow," NASA CR-3970, March 1986.

[3]Dodbele, S. S., Van Dam, C. P., Vijgen, P. M. H. W., and Holmes, B. J., "Shaping of Airplane Fuselages for Minimum Drag," *Journal of Aircraft*, Vol. 24, No. 5, May 1987, pp. 298–304.

[4]Carmichael, B. H., "Underwater Vehicle Drag Reduction through Choice of Shape," AIAA Paper 66-657, June, 1966.

[5]Carmichael, B. H., "Computer Study to Establish the Lower Limit of Length-to-Diameter Rates Advisable for Low Drag Bodies," SID64-1938, North American Aviation, Inc., October, 1964.

[6]Carmichael, B. H., "Underwater Drag Reduction Through Optimal Shape," *Underwater Missile Propulsion*, edited by L. Greiner, Compass Publications, Inc., Arlington, VA, 1966.

[7]Vijgen, P. M. H. W., Dodbele, S. S., Holmes, B. J., and Van Dam, C. P., "Effects of Compressibility on Design of Subsonic Fuselages for Natural Laminar Flow," *Journal of Aircraft*, Vol. 25, No. 9, Sept. 1988, pp. 776–782.

[8]Boltz, E. W., Kenyon, G. C., and Allen, C. Q., "The Boundary-Layer Transition Characteristics of Two Bodies of Revolution, a Flat Plate, and an Unswept Wing in a Low-Turbulence Wind Tunnel," NASA TN D-309, April 1960.

[9]Boltz, E. W., Kenyon, G. C., and Allen, C. Q., "Measurements of Boundary-Layer Transition at Low Speeds on Two Bodies of Revolution in a Low-Turbulence Wind Tunnel," NACA RM A56G17, Sept. 1956.

[10]Vijgen, P. M. H. W., Dodbele, S. S., Pfenninger, W., and Holmes, B. J., "Analysis of Wind-Tunnel Boundary-Layer Transition Experiments on Axisymmetric Bodies at Transonic Speeds Using Compressible Boundary Layer Stability Theory," AIAA Paper 88-0008, 1988.

[11]Smith, A. M. O., "Transition, Pressure Gradient and Stability Theory." IX International Congress for Applied Mechanics, Brussels, Belgium, 1956.

[12]Van Ingen, J. L., "A Suggested Semi-Empirical Method for the Calculation of the Boundary Layer Transition Region," University of Technology, Department of Aerospace Engineering, VTH-74, Delft, The Netherlands, 1956.

[13]Hefner, J. N., and Bushnell, D. M., "Status of Linear Boundary-Layer Stability Theory and the e^n-method, with Emphasis on Swept-Wing Applications," NASA TP-1645, Feb. 1980.

[14]Jaffe, N. A., Okamura, T. T., and Smith, A. M. O., "Determination of Spatial Amplification Factors and their Application to Predicting Transition," *AIAA Journal*, Vol. 8, No. 2, 1970, pp. 301–308.

[15]Bushnell, D. M., Malik, M. R., and Harvey, W. D., "Transition Prediction in External Flows via Linear Stability Theory," IUTAM Symposium Transsonicum III, Gottingen, Germany, May 24–27, 1988.

[16]Malik, M. R., "Instability and Transition in Supersonic Boundary Layers," *Laminar Turbulent Boundary Layers*, edited by: E. M. Uram and H. E. Weber, Energy Resources Technology Conference, New Orleans, LA, Feb. 12–16, 1984.

[17]Granville, P. S., "The Calculation of the Viscous Drag of Bodies of Revolution," David Taylor Model Basin Rept. 849, 1953.

[18]Dodbele, S. S., "Effects of the Forebody Geometry on Subsonic Laminar Boundary Layer Stability," in *Numerical Methods in Laminar and Turbulent Flows*," Vol. 5, Pt. 1, Pineridge Press International, Swansea, Wales, UK, 1987, pp. 902–917.

[19]Vanderplaats, G. N., "CONMIN—A Fortran Program for Constrained Function Minimization," NASA TMX-62282, 1973.

[20]Hall, P. E., and Murray, W., "Quasi-Newton Methods for Unconstrained Optimization," *Journal of Institute of Mathematics and its Applications*, Vol. 9, 1972, pp. 91–108.

[21]Rechenberg, I., "Evolutionsstrategie," Frommann-Holzboog Stuttgast-Bad Cannstatt, Germany.

[22]Maskew, B., "Prediction of Subsonic Aerodynamic Characteristics—A Case for Low-Order Panel Methods," *Journal of Aircraft*, Vol. 19, No. 2, 1982, pp. 157–163.

[23]Harris, J. E., and Blanchard, D. K., "Computer Program for

Solving Laminar, Transitional, or Turbulent Compressible Boundary-Layer Equations for Two-Dimensional and Axisymmetric Flow," NASA TM 83207, Feb. 1982.

[24]Malik, M. R., "COSAL-A Black-Box Compressibility Stability Analysis Code for Transition Prediction in Three-Dimensional Boundary Layers," NASA CR 165925, May 1982.

[25]Gaster, M., "Prediction of Linear Wave Packets in Laminar Boundary-Layers," *AIAA Journal*, Vol. 19, No. 4, 1981, pp. 419–423.

[26]Kuethe, A. M., "On the Stability of Flow in the Boundary-Layer Near the Nose of a Blunt Body," U.S. Air Force Project RAND RM-1972, ASTIA Doc.-150687, 1957.

[27]Morris, P. J., and Byon, W., "The Stability of the Axisymmetric Boundary-Layer on a Circular Cylinder," AIAA Paper 82-1012, 1982.

[28]Floryan, J. M., and Saric, W. S., "Stability of Gortler Vortices in Boundary Layers," *AIAA Journal*, Vol. 20, No. 4, 1982, pp. 316–324.

[29]Hall, P., "The Görtler Vortex Instability Mechanism in Three-Dimensional Boundary-Layers," *Proceedings of the Royal Society of London*, Series A, No. 399, pp. 135–152, 1985.

[30]Shanebrook, J. R., and Sumner, W. J., "Entrainment Theory for Axisymmetric, Turbulent Incompressible Boundary Layers," *Journal of Hydronautics*, Vol. 4, Oct. 1970.

[31]Gërtler, M., "Resistance Experiments on a Systematic Series of Streamlined Bodies for Application to the Design of High-Speed Submarines," David Taylor Model Basin Rept. C-297, April 1950.